

Tau-tubulin kinase 1 enhances prefibrillar tau aggregation and motor neuron degeneration in P301L FTDP-17 tau-mutant mice

Jiqing Xu,¹ Shinji Sato,¹ Satoshi Okuyama,¹ Russell J. Swan, Michael T. Jacobsen, Elena Strunk, and Tsuneya Ikezu²

Department of Pharmacology and Experimental Neuroscience and Center for Neurodegenerative Disorders, University of Nebraska Medical Center, Omaha, Nebraska, USA

ABSTRACT Tau-tubulin kinase-1 (TTBK1) phosphorylates microtubule-associated protein tau at specific serine/threonine residues found in paired helical filaments (PHFs), and its expression is up-regulated in the brain in Alzheimer disease, suggesting its role in tauopathy pathogenesis. To understand the effects of TTBK1 on tauopathy *in vivo*, we have developed bigenic mice overexpressing full-length TTBK1 and the P301L tau mutant. The bigenic mice show enhanced tau phosphorylation at multiple sites (AT8, 12E8, PHF-1, and pS422), tauC3-immunoreactive tau fragmentation, and accumulation of tau aggregates in cortical and hippocampal neurons at 12–13 mo of age. However, the phosphorylated tau aggregates were predominantly sarkosyl soluble and migrated in the light sucrose density fraction after discontinuous sucrose gradient ultracentrifugation, which suggests that they form small oligomers. The bigenic mice show significant locomotor dysfunction as determined by both rotorod and grip strength tests, as well as enhanced loss of motor neurons in the L4-L5 spinal cord. This neuronal dysfunction and degeneration was associated with increased levels of tau oligomers, cyclin-dependent protein kinase 5 activators p35 and p25, and pY216 phosphorylated glycogen synthase kinase 3- β . These data suggest that TTBK1 up-regulation enhances tau phosphorylation and oligomerization, whose toxicity results in enhanced neurodegeneration and locomotor dysfunction in a tauopathy animal model.—Xu, J., Sato, S., Okuyama, S., Swan, R. J., Jacobsen, M. T., Strunk, E., Ikezu, T. Tau-tubulin kinase 1 enhances prefibrillar tau aggregation and motor neuron degeneration in P301L FTDP-17 tau-mutant mice. *FASEB J.* 24, 2904–2915 (2010). www.fasebj.org

Key Words: transgenic mouse model • neurodegeneration • protein kinase • frontotemporal dementia • tauopathy • cyclin-dependent kinase 5

MICROTUBULE-ASSOCIATED CYTOSKELETAL TAU protein has been a focal point in understanding the molecular mechanism of neurofibrillary tangle (NFT) formation through its multiple phosphorylation, monoubiquitina-

tion, limited endoproteolysis of its N- and C-terminal regions, and conformational changes. Neuropathological studies strongly support that NFT formation closely correlates with Alzheimer disease (AD) staging (1). However, recent studies on a transgenic tau mouse (rTg4510) with conditional transgene expression of a tau mutant (P301L tau) genetically linked to the hereditary frontotemporal dementia with parkinsonism linked to chromosome 17 (FTDP-17) suggest that intracellular accumulation of tau, not NFT formation, is responsible for neurodegeneration and cognitive impairment (2). The following studies revealed that new forms of tau aggregates, which are 140- to 170-kDa multimer forms, are accumulated in rTg4510 mice (3). Similarly, granular tau oligomers are also increased in the early stage of tauopathy (Braak I-III) in AD brains (4), which suggests the novel role of tau oligomers (or multimers) for the early stage of neurodegeneration and cognitive impairment. However, the mechanism of tau multimer/oligomer formation was unknown. This study reveals that tau phosphorylation may be one of the mechanisms for the enhanced tau oligomerization.

A number of kinases have been characterized as tau kinases, most notably cyclin-dependent protein kinase 5 (CDK5), glycogen synthase kinase-3 β (GSK3 β), and microtubule affinity regulating kinase (5–9). GSK3 β activity is dually regulated by its autophosphorylation at tyrosine 216 (Y216) for activation and phosphorylation at serine 9 (S9) by Akt for inactivation (10, 11). Association of CDK5 with its neuron-specific regulatory subunit p35 activates its catalytic activity, whereas cleavage of p35 to p25 by specific proteases, such as calpain-1, and formation of CDK5/p25 complexes results in its aberrant activation (8, 12, 13). We have recently identified a new tau kinase, tau tubulin kinase 1 (TTBK1), which is specifically expressed in neurons and can directly phosphorylate tau proteins both *in vitro* and *in vivo* at multiple ser/thr residues that are found on PHF-tau in AD brains (14). TTBK2, a TTBK1

¹ These authors contributed equally to this work.

² Correspondence: 985930 Nebraska Medical Center, Omaha, Nebraska 68198-5930, USA. E-mail: tikezu@unmc.edu
doi: 10.1096/fj.09-150144

isoform, was recently linked to the development of spinocerebellar ataxia type 11 (15), which develops NFT in the brain. These results strongly indicate that TTBK1 and TTBK2 are involved in tau phosphorylation and neurodegeneration.

Because there is currently no transgenic mouse model of TTBK1 or TTBK2 available, we have created transgenic mice (TTBK1-Tg) harboring 57-kb human *TTBK1* genomic DNA, containing entire endogenous promoters, exons, and introns, to reconstitute the physiological expression pattern of the human *TTBK1* gene in mice in order to study the role of TTBK1 in central nervous system (CNS) pathologies (16). TTBK1-Tg mice express an ~8-fold higher level of human TTBK1 as compared to endogenous TTBK1, and TTBK1-Tg expression, driven by its endogenous human genomic promoter, is specific to neurons (subiculum and pyramidal neurons in hippocampus, cortical neurons, and cerebellar Purkinje cells). TTBK1 mice show spatial learning impairment, activation of CDK5 and calpain-1, and down-regulation of *N*-methyl-D-aspartate receptor 2B in a CDK5- and calpain-1-dependent manner, although their locomotor function is intact. Because we did not see robust changes in phosphorylation of endogenous tau protein or its aggregation in TTBK1-Tg mice, we crossed them with JNPL3 mice expressing P301L tau mutant (JNPL3) under the control of the mouse prion protein (PrP) promoter to address the effect of TTBK1 overexpression on the animal model of FTDP-17 in this study. TTBK1/JNPL3 mice develop age-dependent pathology in the CNS, including intraneuronal accumulation of phosphorylated tau, accumulation of sarkosyl-soluble phospho-tau multimers, CDK5 and GSK3 β activation, locomotor dysfunction, and motor neuron degeneration. These data indicate that TTBK1 is involved in phosphorylation-dependent generation of pathogenic tau aggregation *in vivo*.

MATERIALS AND METHODS

Transgenic animal models

All the animal-related procedures were reviewed and approved by the Institutional Animal Care and Use Committee and the University of Nebraska Medical Center. Generation of TTBK1-Tg mice (line 141) harboring human TTBK1 genomic DNA (57 kb) has been previously described (16). The founders in the B6/SJL F1 background were backcrossed to the B6/129 F1 strain (Jackson Laboratories, Bar Harbor, ME, USA) for ≥ 5 generations prior to the study, and non-transgenic (non-Tg) littermates were used for the control group to minimize the effect of background differences. Transgenic JNPL3 mice expressing the P301L mutant of 4-repeat tau without amino-terminal inserts (4R0N; see ref. 17 for tau isoform nomenclature; ref. 18) were backcrossed to the B6/129 F1 strain for ≥ 5 generations and crossed with TTBK1 mice to generate TTBK1, JNPL3, TTBK1/JNPL3, and non-Tg mice.

Immunoblot analysis and antibodies

Proteins were separated by SDS-PAGE, transferred to Immobilon-P membrane (Millipore, Billerica, MA, USA), and

blocked with blocking buffer (SuperBlock with 5% skim milk; Pierce, Rockford, IL, USA). The following antibodies were used for immunoblotting: β -actin mAb (1:10,000 dilution; Sigma-Aldrich, St. Louis, MO, USA); β -tubulin mAb (1:10,000; Abcam, Cambridge, MA, USA); T14 mAb (1:1000; Zymed); tau-5 (1:1000; Invitrogen, Carlsbad, CA, USA); AT8 mAb (phospho-tau Ser-199, Ser-202, and Thr205, 1:500; Innogenetics, Gent, Belgium); PHF-1 mAb (phospho-tau Ser-396 and Ser-404, 1:250; a gift from P. Davies, Albert Einstein College of Medicine, Bronx, NY, USA); 12E8 mAb (phospho-tau Ser-262 and Ser-356, 1:1000; a gift from P. Schubert, Athena Neurosciences Inc., South San Francisco, CA, USA) (19); pS422 (phospho-tau Ser-422, 1:200/1:1000; a gift from A. Delacourte, INSERM, Lille, France) (20), p35/p25 CDK5 activator pAb (C terminus, 1:100; Santa Cruz Biotechnology, Santa Cruz, CA, USA), phospho-GSK3 β mAb (Ser-9, 1:1000, Cell Signaling Technology, Danvers, MA, USA), phospho-GSK3 α/β mAb (phospho-Tyr279/216, 1:1000; Upstate Biotechnology/Millipore, Bedford, MA, USA), GSK3 β pAb (C terminus, 1:2000 Santa Cruz Biotechnology), phospho-neurofilament mAb (pNF, 1:200; Dako, Carpinteria, CA, USA), and TTBK1 mAb (clone F287-1.1-1E9, 13.55 μ g/ml). TTBK1 mAb cross-reacts with human and mouse TTBK1 but not with TTBK2. The luminescent band intensities were quantified by the Phosphoimaging system (Phosphoimager, GE Healthcare/Molecular Dynamics, Sunnyvale, CA, USA) for statistical analyses.

Discontinuous sucrose gradient ultracentrifugation

We applied the method for granular tau oligomer fractionation with minor modifications (4, 21). Briefly, mouse brain hemispheres (12 mo old) were homogenized with a Potter (10 strokes at 1000 *g*) in 3 vol of cold buffer containing 10 mM Tris, pH 7.4; 800 mM NaCl; 1 mM EGTA; and 10% sucrose supplemented with protease inhibitors and then centrifuged at 25,000 *g* for 20 min in a TLA100.4 rotor (Beckman Coulter, Fullerton, CA, USA) at 4°C. Fibrillar tau aggregates were mostly precipitated in the pellet in this procedure. One milliliter of the supernatant was overlaid with a 9-ml discontinuous gradient (50, 45, 40, 35, 30, 25, 20, 15, and 10% sucrose) in a Beckman SW41Ti ultracentrifuge tube. Following centrifugation at 40,000 *g* for 2 h at 23°C, 10 \times 1 ml fractions of the gradient were separated from the bottom of the tube. Fifteen microliters of each fraction was subjected to 10% SDS-PAGE and immunoblotting using AT8 (1:500 dilution; Innogenetics), T14 (1:50, human tau specific; Zymed Laboratories, Burlingame, CA, USA), and Synaptophysin mAbs (1:500, Sigma-Aldrich).

Preparation of brain extracts/spinal cord and tau biochemistry

Brain extracts were prepared according to published protocol (22). Briefly, hemibrains were weighed and homogenized in 3 vol of Tris-buffered saline containing protease and phosphatase inhibitors (25 mM Tris-HCl, pH 7.4; 150 mM NaCl; 1 mM EDTA; 1 mM EGTA; 5 mM sodium pyrophosphate; 30 mM β -glycerophosphate; 30 mM sodium fluoride; 1 mM phenylmethylsulfonyl fluoride). The homogenates were centrifuged in a Beckman TLA 100.4 rotor at 150,000 *g* for 15 min at 4°C. Supernatants were collected as S1 fractions, and the pellets were rehomogenized in 3 vol of salt/sucrose buffer (0.8 M NaCl; 10% sucrose; 10 mM Tris/HCl, pH 7.4; 1 mM EGTA; and 1 mM PMSF) and centrifuged as above. The resultant pellets were discarded, and the supernatants were incubated with sarkosyl (Sigma, 1% final concentration) for 1 h at 37°C. Subsequently, the mixtures were spun in TLA

100.4 rotor at 150,000 *g* for 30 min at 4°C. The supernatants were collected as S2 fractions, while the pellets were collected as P3.

Preparation of spinal cord extracts and immunoblotting for pathological tau species were carried out as reported previously, with modifications (3, 22). Briefly, whole spinal cords of 5-month JNPL3 (4 mice), TTBK1/JNPL3 (4 mice), and non-Tg mice (2 mice) were isolated and quickly frozen on dry ice and stored at -80°C. Each spinal cord was weighed and homogenized in 3 vol of Tris-buffered saline containing protease and phosphatase inhibitors (25 mM Tris-HCl, pH7.4; 150 mM NaCl; 1 mM EDTA; 1 mM EGTA; 5 mM sodium pyrophosphate; 30 mM β-glycerophosphate; 30 mM sodium fluoride; and 1 mM phenylmethylsulfonyl fluoride). The homogenates were ultracentrifuged at 150,000 *g* for 15 min at 4°C, and the supernatants were collected as S1 fractions. A total of 15 μg of an S1 fraction was mixed with an equivalent volume of 2× SDS-sample buffer (Invitrogen), boiled for 5 min, and then loaded on 6% polyacrylamide Tris-glycine gels for SDS-PAGE and immunoblotting. The luminescent band intensities were quantified by the Phosphoimaging system for statistical analyses.

Immunohistochemistry and confocal immunofluorescence microscopy

Immunohistochemistry was performed as described previously (23, 24). Briefly, mice were euthanized with isoflurane and perfused transcardially with 25 ml of ice-cold PBS. The brains were rapidly removed, immersed in freshly depolymerized 4% paraformaldehyde for 48 h, and cryoprotected by successive 24 h immersions in 10, 20, and 30% sucrose in 1× PBS. Fixed, cryoprotected brains were frozen and sectioned in the coronal plane at 30 μm using a cryostat (Leica, Bannockburn, IL, USA) with sections collected serially. Immunohistochemistry was performed using specific antibodies as listed in **Table 1**. Immunostained sections were visualized using Envision Plus (Dako). AT8, 12E8, PHF-1, and pS422 were analyzed by counting positive cell bodies in the hippocampus, parietal, and temporal lobe of the cortex using a Nikon TE-300 microscope (Nikon Instruments, New York, NY, USA).

For fluorescent confocal microscopic imaging, 30-μm spinal cord sections were incubated with 3 primary antibodies [anti-NeuN biotinylated mAb, anti-GFAP mAb, and anti-IBA1 pAb (Wako, Richmond, VA, USA)], washed with washing

buffer, and then incubated with 1:1000 diluted Alexa Fluor647-conjugated anti-mouse IgG (H+L), 1:1000 diluted Alexa Fluor488-conjugated anti-rabbit IgG (H+L) antibodies, and 1:500 diluted Alexa Fluor568-conjugated streptavidin (all from Molecular Probes/Invitrogen) as secondary antibodies. After mounting the sections on slides with Vectashield (Vector Laboratories), the confocal images were captured using a Nikon SweptField slit-scanning confocal microscope (Nikon Instruments) with an ×100 TIRF objective and back-illuminated Cascade 512B CCD camera (Photometrics, Tucson, AZ, USA), with excitation at 488 nm (for IBA1), 568 nm (for NeuN), and 647 nm (for GFAP). The images were pseudo-colored, autocontrasted, and merged as tricolor images (see Fig. 8).

Rotarod test

Testing of motor function using a rotarod device (Rotamex4/8; Columbus Instruments, Columbus, OH, USA) was conducted at 12 mo of age. All mice were pretrained on the apparatus in order for them to reach a stable performance. Each monthly test was performed on the elevated accelerating rotarod (5–30 *g* over 5 min). The time each mouse remained on the rod was recorded automatically. Mice that stayed on the rotarod for > 180 s were considered complete responders; their latencies were recorded as 180 s.

Grip strength test

A grip strength meter (Chatillon; Ametek Inc., Paoli, PA, USA) measured the force exerted by a mouse as it was pulled from a grid by the tail. Grip strength was measured for forelimbs using TTBK1/JNPL3 and JNPL3 mice (*n*=10/group) at 12 mo of age. The measurement was repeated 5 times for both forelimbs and all limbs; the highest score for each animal was obtained.

Motor neuron staining and counting

Spinal cords were dissociated from vertebral columns after being fixed in 10% formalin at 12–13 mo of age. Segments spanning L4–L5 were removed under a dissecting microscope and further fixed with 10% formalin for 4 h, and subsequently frozen after cryoprotection with a series of phosphate-buffered sucrose solu-

TABLE 1. Summary of antibodies used for immunohistochemistry

Antibody	Epitope protein/amino acids	Type	Dilution	Resource
TTBK1	TTBK1 kinase domain	M	1:100	T.I. laboratory
GFAP	Glial fibrillary acidic protein	P	1:2000	Dako (Carpinteria, CA, USA)
IBA1	C-terminal protein	P	1:1000	Wako (Richmond, VA, USA)
Phospho-NF	Phosphorylated neurofilament	M	1:200	Dako
Synaptophysin	Synaptosome preparation	M	1:2000	Sigma-Aldrich (St. Louis, MO, USA)
12E8	tau Ser262 and/or Ser356	M	1:5000	Elan (South San Francisco, CA, USA) P. Davies (Albert Einstein College of Medicine, Bronx, NY, USA)
PHF-1	tau Ser396 and Ser404	M	1:100	Innogenetics (Gent, Belgium)
AT8	tau Ser199, Ser202 and Thr205	M	1:200	A. Delacourte (INSERM, Lille, France)
pS422	tau Ser422	P	1:200	M. Novak (Medical Research Council Laboratory of Molecular Biology, Cambridge, UK)
MN423	tau 306-311 and 321-325	M	1:500	P. Davies
TG3	tau Thr231 and Ser235	M	1:20	L. Binder (Northwestern University, Chicago, IL, USA)
Tau66		M	1:500	L. Binder
TauC3	tau cleaved by caspase3 at Asp421	M	1:500	L. Binder
TauC6	tau cleaved by caspase6	P	1:10,000	A. LeBlanc (McGill University, Montreal, QC, Canada)

M, monoclonal; P, polyclonal.

tions of increasing concentration (15 and 30%). Transverse sections of 30- μ m thickness were stained with the Luxol Fast Blue staining protocol (http://www.ihcworld.com/_protocols/special_stains/fast_blue.htm).

Motor neurons within the ventral horn with identifiable nuclei in L4–L5 were counted in 10 transverse sections from each mouse.

Statistical analysis

Biochemical experiments were repeated 3 times, and all data were normally distributed. In the case of multiple mean comparisons, data were examined by ANOVA, followed by Newman-Keuls (for 1-way ANOVA) or Bonferroni (for 2-way ANOVA) multiple comparison tests using statistics software (Prism 4.0; GraphPad Software, San Diego, CA, USA). In the case of single mean comparison, data were analyzed by Student's *t* test. Values of *P* < 0.05 were regarded as significant.

RESULTS

Expression of the TTBK1 transgene in mouse brain

We have developed a TTBK1 mAb against the catalytic domain of human TTBK1, which detected both endogenous full-length and processed TTBK1 ~ 200 and 80–100 kDa, respectively, in mouse brain (Fig. 1A). TTBK1 undergoes chloroquine-sensitive endoproteolysis to generate a processed form, presumably because of lysosomal processing, but both forms retain kinase activity (25). Both forms of TTBK1 expression were enhanced in the TTBK1/JNPL3 group, whereas transgenic P301L tau expression did not alter endogenous TTBK1 expression at 12–13 mo of age. Transgenic TTBK1 gene expression is specific to the CNS as determined by both Northern and Western blotting of multiple tissues (16). Immunohistochemistry of adult TTBK1/JNPL3 mouse brain identified especially high levels of TTBK1 in the subiculum and external pyramidal layer of the parietal cortex when compared to the same regions in age-matched JNPL3 mice (Fig. 1B), suggesting its role in hippocampal and cortical functions.

Accumulation of phosphorylated tau proteins in TTBK1/JNPL3 mouse brain

Because TTBK1 is known to phosphorylate tau protein, we examined tau phosphorylation in TTBK1/JNPL and age-matched JNPL3 mouse brain at 12–13 mo of age using a panel of anti-phospho-tau specific antibodies. TTBK1/JNPL3 mice exhibit enhanced cytoplasmic accumulation of phospho-tau proteins, indicative of somatodendritic missorting of tau proteins, as compared to the JNPL3 littermates in cortical and hippocampal regions, as detected by AT8, 12E8, PHF-1, and pS422 (Fig. 2A). TTBK1/JNPL3 mice also show accumulation of caspase-3-cleaved tau, as detected by tauC3 (Fig. 2B) (26). However, there was no staining by tauC6 antibody, which detects caspase-6-cleaved tau (data not shown) (27, 28). Quantification of immunostained cells in cortical and hippocampal regions demonstrates a significant increase of AT8, 12E8, PHF-1, and pS422-positive cells in TTBK1/JNPL3 mice as compared to the age-matched JNPL3 littermates (Table 2). These data suggest that TTBK1 enhances accumulation of phosphorylated tau at multiple sites as compared to JNPL3 littermates in 2 different brain regions, hippocampus and cortex. Next, we examined whether the enhanced tau phosphorylation can be seen at an earlier time point. For that purpose, TTBK1/JNPL3 and JNPL3 littermates were subjected to immunohistochemistry at 5–6 mo of age using AT8, CP13, and PHF-1 antibodies (Fig. 3). As expected, the number of immunostained cells by any of the antibodies was much less than 12- to 13-mo-old brain and was mainly localized in the hippocampus. However, immunopositive cells for AT8 and PHF-1 staining are more abundant in TTBK1/JNPL3 brain as compared to JNPL3 littermates, whereas CP13 staining was similar between 2 groups. The AT8⁺ or PHF-1⁺ tau signals were mainly localized in the cytoplasm of pyramidal neurons (Fig. 3, bottom panels). These data suggest that TTBK1 enhances cytoplasmic phospho-tau accumulation as early as 5–6 mo of age.

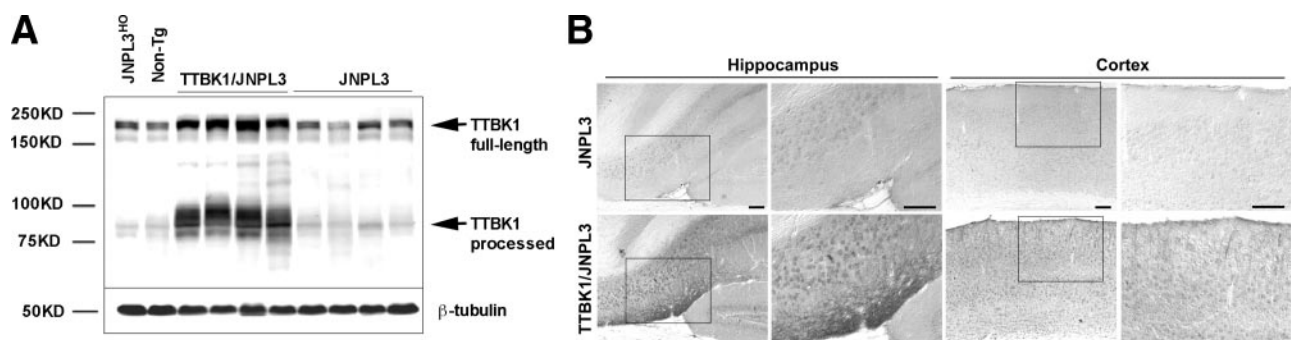


Figure 1. Expression of TTBK1 transgene. A) Cytoplasmic protein samples (S1 fraction, 100 μ g/lane) from TTBK1/JNPL3 and JNPL3 mouse brains (12–13 mo of age) were subjected to 7% SDS-PAGE and immunoblotting for full-length (180–200 kDa) and processed TTBK1 (80–105 kDa) (top panel, arrows) and β -tubulin (bottom panel). JNPL3^{HIO}, age-matched JNPL3 transgene homozygote; Non-Tg, age-matched nontransgenic mouse. B) Coronal brain sections (30 μ m thick) of JNPL3 or TTBK1/JNPL3 mice at 12–13 mo old were immunostained with anti-TTBK1 mAb. Scale bars = 100 μ m.

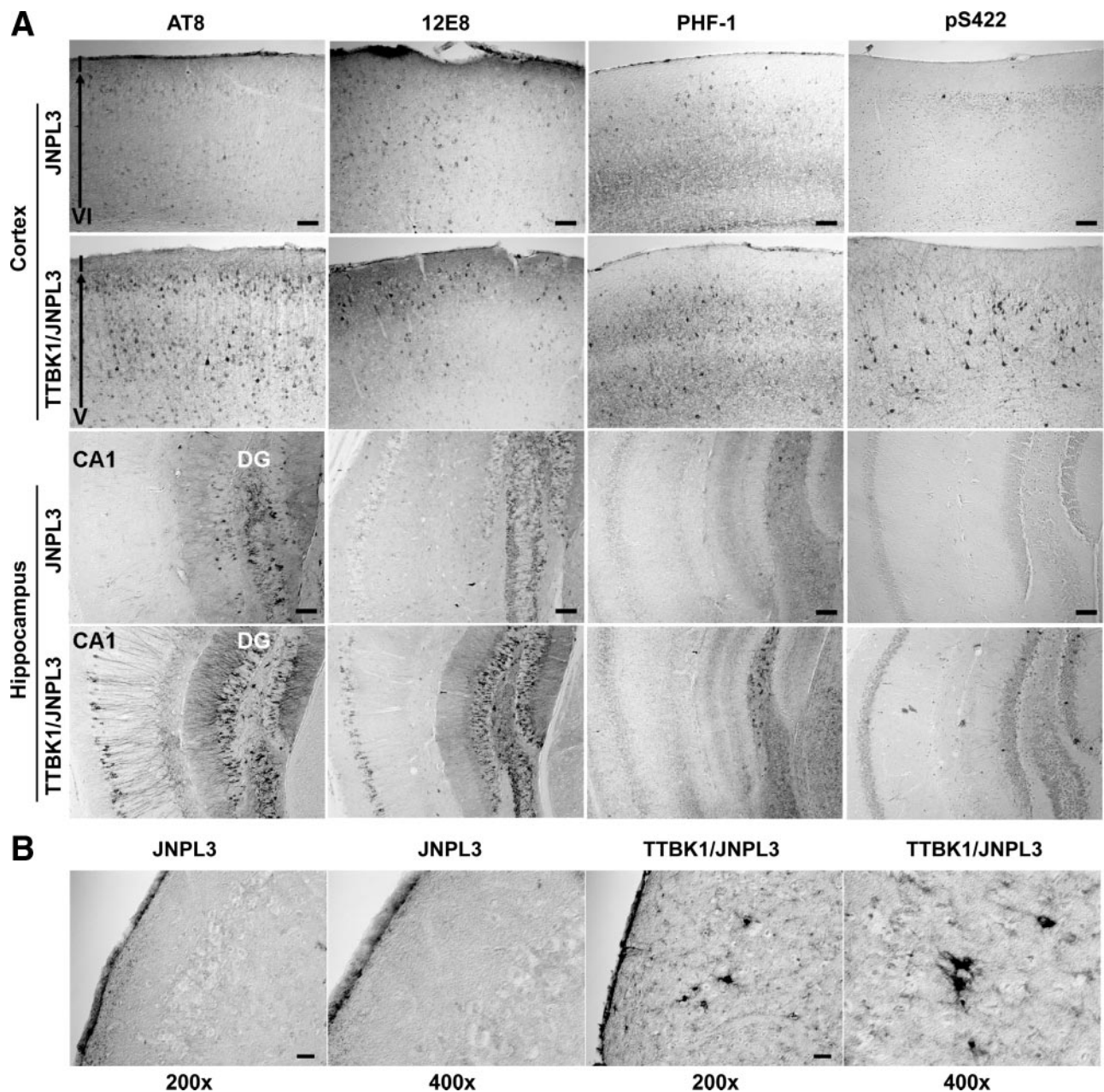


Figure 2. Enhanced phospho-tau and tauC3 staining in TTBK1/JNPL3 mouse brain. *A*) Coronal brain sections (30 μ m thick) of JNPL3 or TTBK1/JNPL3 mice at 12–13 mo old were immunostained with anti-phospho-tau mAb (AT8, 12E8, PHF-1) and pAb (pS422). *B*) Cortical images on tauC3 immunostaining (specific to caspase-3-cleaved tau). Original view: $\times 100$ (*A*); $\times 200$ (*B*, left panels); $\times 400$ (*B*, right panels). Scale bars = 100 μ m (*A*); 50 μ m (*B*).

Accumulation of nonfibrillar form of tau aggregates in TTBK1/JNPL3 mice

The phosphorylation status of the cytoskeletal proteins was also determined by subcellular fractionation of brain samples from the mouse brain at 12–13 mo of age. The brain samples were homogenized in Tris-buffered saline, ultracentrifuged, and the pellets were solubilized in sarkosyl solution. After ultracentrifugation, the supernatants (S2 sarkosyl-soluble fractions) of the brain lysate samples, enriched in polymerized cytoskeletal molecules in the cytoplasm, were tested with immunoblotting of tau and neurofilaments (**Fig. 4A, B**).

Chemiluminescence intensity measurements of the immunoreactive bands demonstrated significant increases in tau phosphorylation at AT8 and 12E8 recognition sites but not in PHF-1 or p-NF sites. However, we have unexpectedly found that the sarkosyl-insoluble fraction (P3) of tau, which represents fibrillar tau aggregates, is significantly reduced in TTBK1/JNPL3 mice as compared to the age-matched JNPL3 littermates (**Fig. 4C, D**) as either the phosphorylated form (AT8 blot, **Fig. 4C**, top panel) or total tau (T14 blot, **Fig. 4C**, bottom panel). We have tested other anti-phospho-tau antibodies, but only AT8 and T14 detected the tau protein in the P3 fraction of TTBK1/JNPL3 mice (data not

TABLE 2. AT8, 12E8, PHF-1, and pS422-positive cell counting

Antibody	Area	JNPL3	TTBK1/JNPL3
AT8	Parietal lobe	149.2 ± 12.29	168.4 ± 9.76
	Temporal lobe	40.04 ± 2.93	115.9 ± 7.4***
	Hippocampus	198.2 ± 16.88	284.2 ± 26.24**
12E8	Parietal lobe	39.8 ± 4.54	167.6 ± 14.51***
	Temporal lobe	11.28 ± 1.51	79.38 ± 7.06***
	Hippocampus	158.4 ± 20.7	319.0 ± 19.25***
PHF-1	Parietal lobe	61.13 ± 4.99	95.13 ± 9.05**
	Temporal lobe	8.34 ± 1.07	35.11 ± 4.38***
	Hippocampus	120.6 ± 7.56	140.2 ± 11.66
pS422	Parietal lobe	3.18 ± 1.1	7.44 ± 2.01
	Temporal lobe	10.94 ± 2.66	63.76 ± 19.09**
	Hippocampus	1.29 ± 0.44	6.28 ± 2.07**

** $P < 0.01$, *** $P < 0.001$; Student's t test.

shown). These data suggest that cytoplasmic accumulation of phospho-tau in TTBK1/JNPL3 mice was not occurring as fibrillar tau aggregates. Recent studies suggest that compartmentalization of fibrillar tau does not correlate with memory loss or neurodegeneration (2), and formation of tau multimers (or oligomers) was correlated with spatial memory impairment (3). Thus, it is possible that TTBK1 expression shifts the tau aggregation status from the fibrillar form to pathological tau multimer species in the TTBK1/JNPL3 mouse brain. To test this possibility, we subjected the mouse brain homogenate samples to sucrose gradient ultracentrifugation in order to purify the granular tau oligomers as described (21). Using this technology, granular tau oligomers can be collected in the top fractions, while the majority of the fibrillar tau aggregates were precipitated after the first centrifugation at 25,000 g prior to the application of the supernatant to the sucrose gradient ultracentrifugation (Fig. 5). A trace amount of remaining fibrillar tau can be observed in the 30–40% fractions in JNPL3 mouse brain, which was not quantitative because the majority of the fibrillar tau has already been precipitated prior to the loading of the supernatant to the sucrose gradient ultracentrifugation (see Materials and Methods). Using this technique, we

detected an enhanced level of AT8-positive tau oligomers, which migrate above the 250 kD or around the 50-kD molecular marker, in the 10–20% sucrose fraction. Because the originally monomeric tau and disaggregated tau oligomers that migrated around the 50-kD molecular marker were virtually indistinguishable, we evaluated tau oligomers that migrated at the >250-kD marker, which are abundant in TTBK1/JNPL3 mice as compared to age-matched JNPL3 mice (Fig. 5, phospho-tau panels). Tau oligomers were also detected by T14 antibody (Fig. 5, total tau bottom panels). These data demonstrate the enhancement of tau multimer formation and its phosphorylation in TTBK1/JNPL3 mice.

TTBK1 up-regulates p25 and p35 subunits of CDK5 complexes and the activated form of GSK3 β

Phosphorylation of tau at multiple ser/thr residues in the TTBK1/JNPL3 mouse brain includes additional sites other than the identified phosphorylation sites (Ser-198, 199, 292, and 422) through direct phosphorylation of tau protein by TTBK1 *in vitro*. This suggests that other tau kinases are activated by TTBK1 expression. In the previous study, we characterized the up-

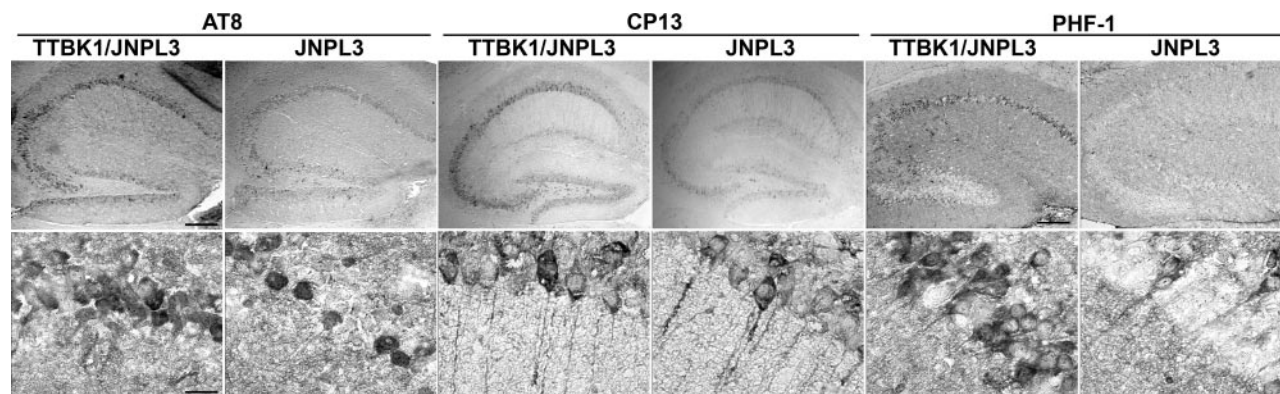


Figure 3. Phospho-tau staining in young TTBK1/JNPL3 mouse brain. Coronal brain sections (30 μm thick) of JNPL3 or TTBK1/JNPL3 mice at 5–6 mo old ($n=6/\text{group}$) were immunostained with anti-phospho-tau mAb (AT8, CP13, PHF-1) and DAB; representative images are shown at lower magnification for the hippocampal region (top panel; $\times 40$) and high-power magnification for the CA1 pyramidal region (bottom panel; $\times 1000$). Scale bars = 200 μm (top panel); 10 μm (bottom panel).

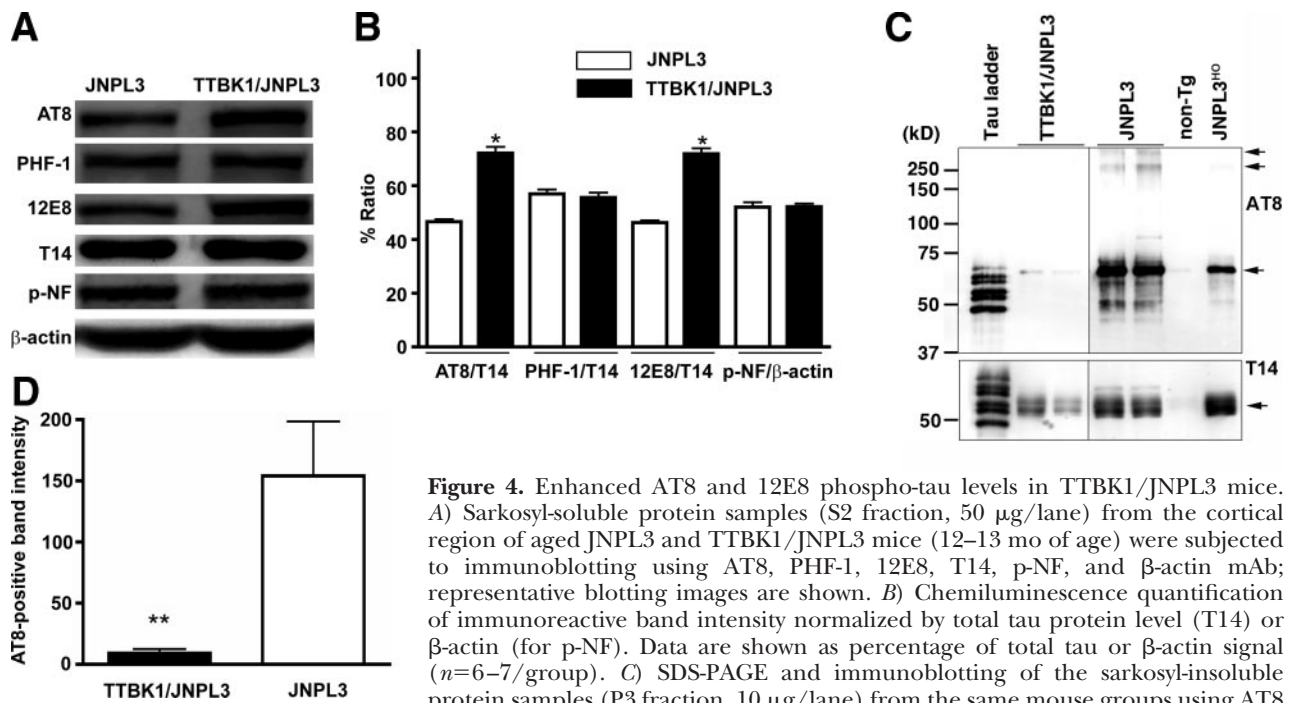


Figure 4. Enhanced AT8 and 12E8 phospho-tau levels in TTBK1/JNPL3 mice. **A)** Sarkosyl-soluble protein samples (S2 fraction, 50 μ g/lane) from the cortical region of aged JNPL3 and TTBK1/JNPL3 mice (12–13 mo of age) were subjected to immunoblotting using AT8, PHF-1, 12E8, T14, p-NF, and β -actin mAb; representative blotting images are shown. **B)** Chemiluminescence quantification of immunoreactive band intensity normalized by total tau protein level (T14) or β -actin (for p-NF). Data are shown as percentage of total tau or β -actin signal ($n=6-7$ /group). **C)** SDS-PAGE and immunoblotting of the sarkosyl-insoluble protein samples (P3 fraction, 10 μ g/lane) from the same mouse groups using AT8 (top panel) or T14 (bottom panel) with tau ladder. Non-Tg and JNPL3^{H10} represent age-matched nontransgenic mice (negative control) and tau transgenic homozygous mice (positive control). Top panel: AT8 immunoblotting; arrows indicate 2 phospho-tau multimer bands >250 kD and AT8-positive tau between the 2N4R and 2N3R tau standards. Tau ladder bands (from top): 2N4R, 2N3R, 1N4R, 1N3R, 0N4R, and 0N3R. Bottom panel: T14 immunoblotting; arrow indicates total tau between the 1N4R and 0N4R tau standards. **D)** Chemiluminescence quantification of AT8 immunoreactive band intensity in P3 fraction ($n=4$ /group). * $P < 0.05$, ** $P < 0.01$; Student's *t* test.

regulation of CDK5 activators p25 and p35 and enhanced activity of p35- or p25-associated CDK5 activity in TTBK1 mouse brain *in vivo* and in tissue culture (16). Accordingly, we observed enhanced tau phosphorylation at AT8 and PHF-1 sites, which are phosphorylated by GSK3 β and CDK5, respectively (29, 30). Thus, we investigated whether other tau kinases (CDK5 and GSK3 β) were activated by TTBK1 expression in JNPL3 mouse brain. TTBK1/JNPL3 mice show enhanced levels of p25, p35, Tyr 216-phosphorylated GSK3 β (pY216 GSK3 β , an activated form of GSK3 β), and Tyr 279-phosphorylated GSK3 α (pY279 GSK3 α , an activated form of GSK3 α ; Fig. 6A). These were up-regulated with statistical significance in TTBK1/JNPL3 mouse brain as compared to age-matched JNPL3 mice (Fig. 6B, C). On the other hand, there was no difference in the amount of Ser-9-phosphorylated GSK3 β (pS9 GSK3 β , an inactivated form of GSK3 β , Fig. 6A, C). These data suggest that both CDK5 and GSK3 β activities are up-regulated, which may lead to the enhanced tau phosphorylation in TTBK1/JNPL3 mouse brain.

Impaired locomotor function and enhanced motor neuron degeneration and tau phosphorylation in the spinal cord of TTBK1/JNPL3 mice

TTBK1/JNPL3 mice also show a significantly shorter retention time on the accelerating rotarod and a reduction in forelimb grip strength as compared to JNPL3 mice (Fig. 7A, B), suggesting locomotor and neuromus-

cular dysfunction. On the other hand, TTBK1 and non-Tg mice performed equally well on rotarod tests (16), which suggests that this locomotor dysfunction is not directly mediated by TTBK1 expression but rather through a modification of tauopathy by TTBK1.

Because we observed significant locomotor dysfunction and reduction of forelimb grip strength in TTBK1/JNPL3 mice, we examined the neuropathology of motor neurons in the anterior horns of spinal cord at the L4–L5 region. Multifluorescence laser-scanning confocal microscopic imaging of this region demonstrates enhanced IBA1-positive cell accumulation, indicative of microgliosis, in TTBK1/JNPL3 mice and reduction of NeuN-positive neuronal cell bodies in JNPL3 and TTB1/JNPL3 mice but not in TTBK1 or non-Tg mice (Fig. 8A). GFAP-positive astrocytes accumulated in TTBK1, JNPL3, and TTBK1/JNPL3 mice, indicating astrogliosis in these groups. Quantification of α and γ -motor neurons in the anterior horns of L4–L5 spinal cord segments by fast blue and hematoxylin staining of spinal cord sections demonstrated a significantly reduced number of motor neurons in TTBK1/JNPL3 mice as compared to the age-matched JNPL3 mice (Fig. 8B), indicating motor neuron degeneration by TTBK1 expression in JNPL3 mice.

We have further tested whether this motor neuron degeneration is due to enhanced tau phosphorylation and aggregation in the spinal cord. A recent study on rTg4510 and JNPL3 mice demonstrated that oligomeric tau can be detected in the spinal cord protein

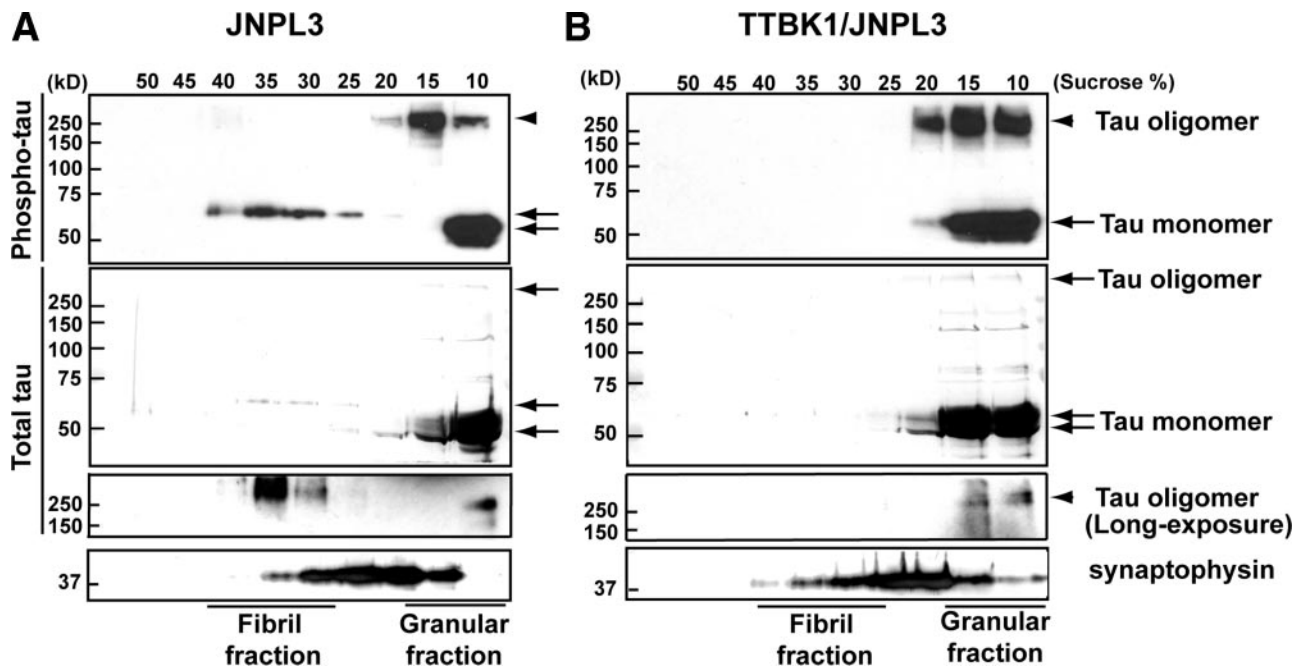


Figure 5. Increased prefibrillar phospho-tau aggregates in TTBK1/JNPL3 mouse brain. Brain homogenates from aged JNPL3 (A) and TTBK1/JNPL3 (B) at 12–13 mo of age were subjected to discontinuous sucrose gradient ultracentrifugation; each fraction (10–50% in 5% increments) was subjected to AT8 (top panel), T14 (2 middle panels), and synaptophysin (bottom panel) immunoblotting. Arrowheads indicate phospho-tau multimer band (>250 kD). Arrows indicate monomeric phospho-tau (top panels) or total tau (middle panel). Synaptophysin is a marker of synaptic vesicles and indicator of the sucrose gradient, which migrates at ~15–25% sucrose.

extract (S1 fraction after ultracentrifugation) of JNPL3 mice (3). Using the same protocol, we could observe that tau oligomers migrated around 170 and 140 kDa molecular weight in the protein extract isolated from the spinal cord of 5- to 6-mo-old JNPL3 and TTBK1/JNPL3 littermates, which were immunoreactive to AT8, 12E8, pS422, and PHF-1 anti-phospho-tau mAbs (Fig.

8C) but not to AT100 or CP13 (data not shown). Protein extracts from the spinal cord of age-matched non-Tg show no oligomeric tau species (data not shown). The immunoreactive band intensities were measured and normalized against β -actin immunoreactivity, and the TTBK1/JNPL3 mouse spinal cord protein extract had significantly higher levels of AT8, 12E8,

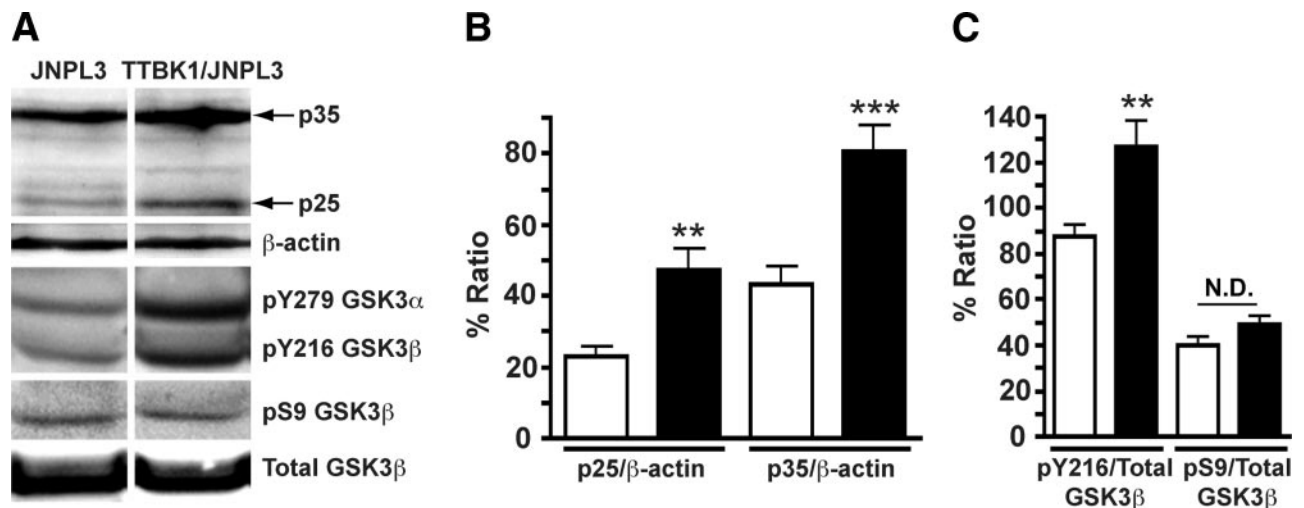


Figure 6. Elevated p25 and p35 subunits of CDK5 complexes and GSK3 β phosphorylation in TTBK1/JNPL3 mouse brain. A) Protein samples (50 μ g/lane) from JNPL3 and TTBK1/JNPL3 mouse cortical region ($n=6$ /group, 12–13 mo of age) were subjected to SDS-PAGE and immunoblotting using anti-p35/p25 pAb, anti- β -actin mAb, anti-phospho-GSK3 α / β pAb (pY279/pY216), anti-phospho-GSK3 β pAb (pS9), or anti-GSK3 β pAb. B, C) Chemiluminescence quantification of immunoreactive bands and presentation as percentage p25/ β -actin or percentage p35/ β -actin (B) or percentage pY216 GSK3 β /total GSK3 β or percentage pS9 GSK3 β /total GSK3 β (C). ** $P < 0.01$, *** $P < 0.001$; Student's t test.

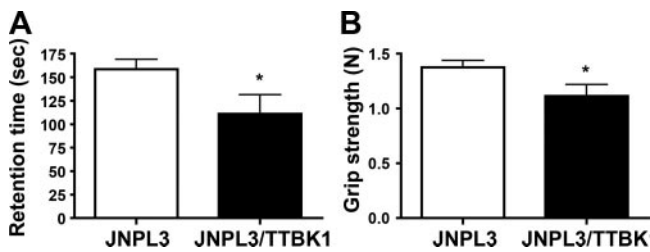


Figure 7. Locomotor function and grip strength in TTBK1/JNPL3 mice. Rotarod (A) and forelimb grip test (B) of JNPL3 (open columns) and TTBK1/JNPL3 mice (solid columns, $n=10$ /group) at 12 mo of age. * $P < 0.05$; Student's t test.

and pS422-immunoreactive tau oligomers as compared to JNPL3 mice, whereas PHF-1-immunoreactive tau oligomers and tau-5-immunoreactive 55kDa tau monomers were unchanged (Fig. 8D). These data collectively suggest that TTBK1 expression enhances accumulation of phosphorylated tau oligomers, which are significantly phosphorylated at TTBK1 phosphorylation sites (AT8 and pS422). To determine whether CDK5 activity is enhanced in the spinal cord of TTBK1/JNPL3 mice, we immunoprecipitated CDK5 activator p35 and performed an *in vitro* kinase assay of coprecipitated CDK5 using histone H1 as a substrate as described (16). The CDK5 activity of the spinal cord was significantly weaker than that of brain extract in our previous study, and there was no difference in p35-associated CDK5 activity between TTBK1/JNPL3 and JNPL3 (data not shown), consistent with the result of the PHF-1 immunoreactivity (Fig. 8D).

DISCUSSION

Tau aggregation and NFT formation are preceded by A β deposition in both clinical and preclinical neuropathological studies (31, 32), and, because the tau gene has not been linked to the familial AD pedigree, tauopathy has been regarded as secondary to A β deposition in the AD pathogenesis. However, the possibility of using it as a therapeutic target has grown more important after recent unsuccessful reports on the phase II trial of A β vaccination in AD patients, which show successful A β removal from brain but a lack of beneficial effects on disease progression (33). This suggests that although A β aggregation or deposition may initiate the AD pathology and symptoms, it may not be an effective target for therapy. Although early transgenic mouse models of FTDP-17 (such as JNPL3) failed to develop cortical or hippocampal neurodegeneration (34), recent models show progressive neurodegeneration and memory loss (35, 36), suggesting its direct role on neurodegeneration. These studies suggest that reduction of tau expression or its phosphorylation by other tau kinases may have a therapeutic potential, although a more specific inhibitor has to be developed for targeting such kinases.

TTBK1-mediated tau phosphorylation, somatodendritic missorting, and multimer formation

Our study demonstrates that overexpression of TTBK1 leads to accumulation of phospho-tau in neuronal cell bodies of the cortex and hippocampus. Intense accumu-

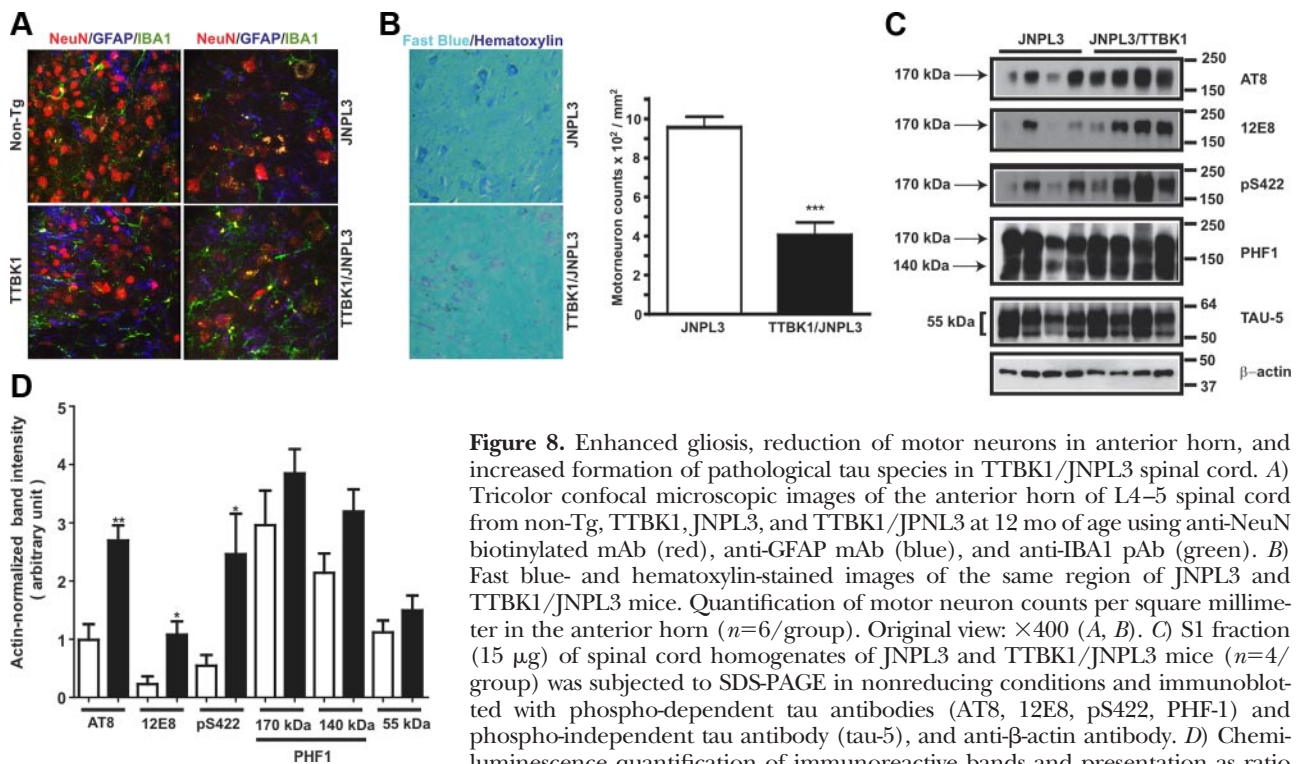


Figure 8. Enhanced gliosis, reduction of motor neurons in anterior horn, and increased formation of pathological tau species in TTBK1/JNPL3 spinal cord. A) Tricolor confocal microscopic images of the anterior horn of L4–5 spinal cord from non-Tg, TTBK1, JNPL3, and TTBK1/JNPL3 at 12 mo of age using anti-NeuN biotinylated mAb (red), anti-GFAP mAb (blue), and anti-IBA1 pAb (green). B) Fast blue- and hematoxylin-stained images of the same region of JNPL3 and TTBK1/JNPL3 mice. Quantification of motor neuron counts per square millimeter in the anterior horn ($n=6$ /group). Original view: $\times 400$ (A, B). C) S1 fraction (15 μ g) of spinal cord homogenates of JNPL3 and TTBK1/JNPL3 mice ($n=4$ /group) was subjected to SDS-PAGE in nonreducing conditions and immunoblotted with phospho-dependent tau antibodies (AT8, 12E8, pS422, PHF-1) and phospho-independent tau antibody (tau-5), and anti- β -actin antibody. D) Chemiluminescence quantification of immunoreactive bands and presentation as ratio over β -actin band intensity. * $P < 0.05$, ** $P < 0.01$, *** $P < 0.001$; Student's t test.

lation of phospho-tau in pyramidal and granular layers in the hippocampus may be an indication of enhanced memory impairment in TTBK1/JNPL3 mice. Enhanced tau phosphorylation at AT8 and pS422 recognition sites is indicative of TTBK1-mediated phosphorylation, as determined by a previous study (25). TTBK1 expression also enhances generation of tau multimers, which are increased in early stages of AD brain (Braak I-III) and different animal models (rTg4510) (3, 4). The approximate molecular mass of the tau multimer differs in reports (~40 mers or 2200 kDa in AD brain, 140–170 kDa in rTg4510 and JNPL3 mice, and >250 kDa in TTBK1/JNPL3 mice). This could be due to differences in the status of tau phosphorylation and other post-translational modifications, sample preparation conditions, or SDS-PAGE conditions. Indeed, the differences in the buffers are significant as the sucrose gradient buffer in the protocol that we adopted contains a high concentration of salt (800 mM NaCl) and sucrose (10–50%, depending on the fraction). This condition may potentially stabilize the tau oligomers in the presence of SDS and high temperature, preventing the disaggregation of the tau oligomers in the SDS sampling process. The reduction of fibrillar tau may also be due to its enhanced phosphorylation at AT8 and PHF-1 sites (pS202/T205, pS396/S404), which are susceptible to heat shock protein 90-induced proteasomal tau clearance (37, 38).

CDK5 and GSK3 β activation

The findings of enhanced p35 (or p25 and p35) levels in TTBK1/JNPL3 mouse brain are consistent with enhanced CDK5 activity associated with p35/p25 in TTBK1 mice due to up-regulation of both p35 and p25 (16). However, this could be restricted to brain because we did not see enhanced p35-associated CDK5 activity in the spinal cord of TTBK1/JNPL3 mice as compared to JNPL3 littermates in this study (data not shown). The elevated level of pY216 GSK3 β in TTBK1/JNPL3 mice was not observed in TTBK1 mice, suggesting that transgene tau mutant expression attribute to the GSK3 β activation. Tau accumulation itself could activate GSK3 β . Indeed, pY216 GSK3 β -expression was detected in NFT-bearing cells in aged JNPL3 mice (39). This is not accompanied by a reduction in inhibitory phosphorylation of GSK3 β at S9, suggesting that the GSK3 β activation may be mediated by autophosphorylation or other tyrosine kinases (such as fyn- and proline-rich tyrosine kinase 2) at Y216 but not through suppression of the S9 phosphorylating kinases, such as Akt and protein kinase A and C (10, 11, 40–44). Similar observations are also found in other models where transgenic expression of an APP mutant activated both GSK3 α and GSK3 β by increasing the levels of p279/216 GSK3 without affecting pS9/21 GSK3 (45). Fyn activation has been documented in NFT-containing neurons in AD and JNPL3 mouse brains (46, 47), which suggests fyn-mediated GSK3 β activation by tau accumulation and which may be further augmented by TTBK1. In addition, this GSK3 β activation may also explain the

activation of caspase 3 and formation of tauC3-positive tau accumulation in the cortical region of TTBK1/JNPL3 mice, which is similar to the previous report (48). Intriguingly, the pY279 GSK3 α expression was also elevated in TTBK1/JNPL3 mice, yet the mechanism and significance of this activation are unclear.

Motor impairment

Aged TTBK1/JNPL3 mice show multiple signs of locomotor and neuromuscular dysfunctions, which are evident in shorter retention on the rotarod, reduced grip strength, gait disturbance, and tremor at a resting posture. We did not observe any of these phenotypes in TTBK1 mice at the same age, indicating that these are mediated through tau modifications rather than a direct TTBK1 effect. Our data also indicate that PNS neurons may be more susceptible to aggregated tau toxicity, which can be enhanced by TTBK1-induced tau phosphorylation. The presence of hyperphosphorylated tau in the spinal cord raises the possibility that spinal cord motor neuron dysfunction accounts for the locomotor dysfunction in the TTBK1/JNPL3 mice. More study will be necessary to understand how TTBK1 enhances tau accumulation in the spinal cord, which leads to neuroinflammation and motor neuron loss.

Neuronal cell loss and astrogliosis

TTBK1/JNPL3 mice displayed other features of neuropathology, such as loss of neurons and astrogliosis in spinal cords, which are analogous to other FTDP tau mutant models (18). Accordingly, we observed TTBK1-induced enhancement of motor neuron degeneration as well as oligomerized tau aggregates phosphorylated at multiple Ser/Thr sites, including AT8, 12E8, and pS422, in the spinal cords of TTBK1/JNPL3 mice. Our mice displayed GFAP-positive cells in the spinal cord, demonstrating that TTBK1 expression induces an inflammatory response. TTBK1-induced tau protein accumulation might down-regulate cell surface expression of antiinflammatory molecules, such as CD200, on neuronal surfaces and enhance neuroinflammation, leading to neuronal cell loss. This is significant because recent studies report that microglial activation precedes tau aggregation in P301S tau mice (35), and that such neuroinflammation may be the cause rather than the result of tauopathy. Further study will be necessary to understand how neuronal TTBK1 expression enhances neuroinflammation in this model.

In summary, to the best of our knowledge, this is the first comprehensive biochemical, behavioral, and neuropathological study to report that the TTBK gene family can modulate the FTDP-17-linked tau mutant mouse phenotype. However, these findings are demonstrated by overexpression of both TTBK1 and FTDP-linked tau mutants, and so we have to be cautious about the potential dose dependency on the mouse phenotype and its clinical relevance. Our

findings may be relevant to understanding the mechanism of how TTBK1 modulates tau multimer formation, neuroinflammation, neurodegeneration, and locomotor dysfunction. Regulation of TTBK1 activity may be a therapeutic target of AD, FTD, and other tauopathy disorders. **FJ**

The authors thank D. Morgan for the consultation in spatial learning tests; A. Takashima for the consultation in sucrose gradient fractionation of tau oligomers; P. Davies (Albert Einstein College of Medicine, Bronx, NY, USA) for PHF-1 and TG2 antibodies; A. Delacourte (INSERM, Lille, France) and M. Hasegawa (University of Tokyo, Tokyo, Japan) for pS422 antibody; P. Schubert (Athena Neurosciences Inc., South San Francisco, CA, USA) for 12E8 antibody; L. Binder (Northwestern University, Chicago, IL, USA) and M. Novak (Medical Research Council Laboratory of Molecular Biology, Cambridge, UK) for tau66, tauC3, and MN423 antibodies; A. LeBlanc (McGill University, Montreal, QC, Canada) for tauC6 antibody; J. Davis (University of Nebraska Medical Center, Omaha, NE, USA) for GSK3 antibodies; and M. Marquardt, K. Estes, and T. Smith for manuscript editing. This work was supported by University of Nebraska Medical Center Faculty Retention Fund (T.I.), John Douglas French Alzheimer's Foundation (S.S.), and Vada Oldfield Alzheimer's Research Awards (S.S. and T.I.).

REFERENCES

- Braak, H., and Braak, E. (1995) Staging of Alzheimer's disease-related neurofibrillary changes. *Neurobiol. Aging* **16**, 271–278; discussion 278–284
- Santacruz, K., Lewis, J., Spire, T., Paulson, J., Kotilinek, L., Ingelsson, M., Guimaraes, A., DeTure, M., Ramsden, M., McGowan, E., Forster, C., Yue, M., Orme, J., Janus, C., Mariash, A., Kuskowski, M., Hyman, B., Hutton, M., and Ashe, K. H. (2005) Tau suppression in a neurodegenerative mouse model improves memory function. *Science* **309**, 476–481
- Berger, Z., Roder, H., Hanna, A., Carlson, A., Rangachari, V., Yue, M., Wszolek, Z., Ashe, K., Knight, J., Dickson, D., Andorfer, C., Rosenberry, T. L., Lewis, J., Hutton, M., and Janus, C. (2007) Accumulation of pathological tau species and memory loss in a conditional model of tauopathy. *J. Neurosci.* **27**, 3650–3662
- Maeda, S., Sahara, N., Saito, Y., Murayama, S., Ikai, A., and Takashima, A. (2006) Increased levels of granular tau oligomers: an early sign of brain aging and Alzheimer's disease. *Neurosci. Res.* **54**, 197–201
- Ishiguro, K., Omori, A., Takamatsu, M., Sato, K., Arioka, M., Uchida, T., and Imahori, K. (1992) Phosphorylation sites on tau by tau protein kinase I, a bovine derived kinase generating an epitope of paired helical filaments. *Neurosci. Lett.* **148**, 202–206
- Arioka, M., Tsukamoto, M., Ishiguro, K., Kato, R., Sato, K., Imahori, K., and Uchida, T. (1993) Tau protein kinase II is involved in the regulation of the normal phosphorylation state of tau protein. *J. Neurochem.* **60**, 461–468
- Imahori, K., and Uchida, T. (1997) Physiology and pathology of tau protein kinases in relation to Alzheimer's disease. *J. Biochem. (Tokyo)* **121**, 179–188
- Patrick, G. N., Zukerberg, L., Nikolic, M., de la Monte, S., Dikkes, P., and Tsai, L. H. (1999) Conversion of p35 to p25 deregulates Cdk5 activity and promotes neurodegeneration. *Nature* **402**, 615–622
- Drewes, G., Ebner, A., Preuss, U., Mandelkow, E. M., and Mandelkow, E. (1997) MARK, a novel family of protein kinases that phosphorylate microtubule-associated proteins and trigger microtubule disruption. *Cell* **89**, 297–308
- Lochhead, P. A., Kinstrie, R., Sibbet, G., Rawjee, T., Morrice, N., and Cleghon, V. (2006) A chaperone-dependent GSK3beta transitional intermediate mediates activation-loop autophosphorylation. *Mol. Cell* **24**, 627–633
- Cross, D. A., Alessi, D. R., Cohen, P., Andjelkovich, M., and Hemmings, B. A. (1995) Inhibition of glycogen synthase kinase-3 by insulin mediated by protein kinase B. *Nature* **378**, 785–789
- Tsai, L. H., Delalle, I., Caviness, V. S., Jr., Chae, T., and Harlow, E. (1994) p35 is a neural-specific regulatory subunit of cyclin-dependent kinase 5. *Nature* **371**, 419–423
- Lee, M. S., Kwon, Y. T., Li, M., Peng, J., Friedlander, R. M., and Tsai, L. H. (2000) Neurotoxicity induces cleavage of p35 to p25 by calpain. *Nature* **405**, 360–364
- Sato, S., Tatebayashi, Y., Akagi, T., Chui, D. H., Murayama, M., Miyasaka, T., Planel, E., Tanemura, K., Sun, X., Hashikawa, T., Yoshioka, K., Ishiguro, K., and Takashima, A. (2002) Aberrant tau phosphorylation by glycogen synthase kinase-3beta and JNK3 induces oligomeric tau fibrils in COS-7 cells. *J. Biol. Chem.* **277**, 42060–42065
- Houlden, H., Johnson, J., Gardner-Thorpe, C., Lashley, T., Hernandez, D., Worth, P., Singleton, A. B., Hilton, D. A., Holton, J., Revesz, T., Davis, M. B., Giunti, P., and Wood, N. W. (2007) Mutations in TTBK2, encoding a kinase implicated in tau phosphorylation, segregate with spinocerebellar ataxia type 11. *Nat. Genet.* **39**, 1434–1436
- Sato, S., Xu, J., Okuyama, S., Martinez, L. B., Walsh, S. M., Jacobsen, M. T., Swan, R. J., Schlautman, J. D., Ciborowski, P., and Ikezu, T. (2008) Spatial learning impairment, enhanced CDK5/p35 activity, and downregulation of NMDA receptor expression in transgenic mice expressing tau-tubulin kinase 1. *J. Neurosci.* **28**, 14511–14521
- Tatebayashi, Y., Miyasaka, T., Chui, D. H., Akagi, T., Mishima, K., Iwasaki, K., Fujiwara, M., Tanemura, K., Murayama, M., Ishiguro, K., Planel, E., Sato, S., Hashikawa, T., and Takashima, A. (2002) Tau filament formation and associative memory deficit in aged mice expressing mutant (R406W) human tau. *Proc. Natl. Acad. Sci. U. S. A.* **99**, 13896–13901
- Lewis, J., McGowan, E., Rockwood, J., Melrose, H., Nacharaju, P., Van Slegtenhorst, M., Gwinn-Hardy, K., Paul Murphy, M., Baker, M., Yu, X., Duff, K., Hardy, J., Corral, A., Lin, W. L., Yen, S. H., Dickson, D. W., Davies, P., and Hutton, M. (2000) Neurofibrillary tangles, amyotrophy and progressive motor disturbance in mice expressing mutant (P301L) tau protein. *Nat. Genet.* **25**, 402–405
- Seubert, P., Mawal-Dewan, M., Barbour, R., Jakes, R., Goedert, M., Johnson, G. V., Litsky, J. M., Schenk, D., Lieberburg, I., Trojanowski, J. Q., and Lee, V. M.-Y. (1995) Detection of phosphorylated Ser262 in fetal tau, adult tau, and paired helical filament tau. *J. Biol. Chem.* **270**, 18917–18922
- Bussiere, T., Hof, P. R., Mailliot, C., Brown, C. D., Cailliet-Boudin, M. L., Perl, D. P., Buee, L., and Delacourte, A. (1999) Phosphorylated serine422 on tau proteins is a pathological epitope found in several diseases with neurofibrillary degeneration. *Acta Neuropathol.* **97**, 221–230
- Maeda, S., Sahara, N., Saito, Y., Murayama, M., Yoshiike, Y., Kim, H., Miyasaka, T., Murayama, S., Ikai, A., and Takashima, A. (2007) Granular tau oligomers as intermediates of tau filaments. *Biochemistry* **46**, 3856–3861
- Sahara, N., Lewis, J., DeTure, M., McGowan, E., Dickson, D. W., Hutton, M., and Yen, S. H. (2002) Assembly of tau in transgenic animals expressing P301L tau: alteration of phosphorylation and solubility. *J. Neurochem.* **83**, 1498–1508
- Yamamoto, M., Kiyota, T., Horiba, M., Buescher, J. L., Walsh, S. M., Gendelman, H. E., and Ikezu, T. (2007) Interferon-gamma and tumor necrosis factor-alpha regulate amyloid-beta plaque deposition and beta-secretase expression in Swedish mutant APP transgenic mice. *Am. J. Pathol.* **170**, 680–692
- Yamamoto, M., Horiba, M., Buescher, J. L., Huang, D., Gendelman, H. E., Ransohoff, R. M., and Ikezu, T. (2005) Overexpression of monocyte chemoattractant protein-1/CCL2 in beta-amyloid precursor protein transgenic mice show accelerated diffuse beta-amyloid deposition. *Am. J. Pathol.* **166**, 1475–1485
- Sato, S., Cerny, R. L., Buescher, J. L., and Ikezu, T. (2006) Tau-tubulin kinase 1 (TTBK1), a neuron-specific tau kinase candidate, is involved in tau phosphorylation and aggregation. *J. Neurochem.* **98**, 1573–1584
- Gamblin, T. C., Chen, F., Zambrano, A., Abrahams, A., Lagalwar, S., Guillozet, A. L., Lu, M., Fu, Y., Garcia-Sierra, F., LaPointe, N., Miller, R., Berry, R. W., Binder, L. I., and Cryns, V. L. (2003) Caspase cleavage of tau: linking amyloid and neurofibrillary tangles in Alzheimer's disease. *Proc. Natl. Acad. Sci. U. S. A.* **100**, 10032–10037

27. Albrecht, S., Bourdeau, M., Bennett, D., Mufson, E. J., Bhattacharjee, M., and LeBlanc, A. C. (2007) Activation of caspase-6 in aging and mild cognitive impairment. *Am. J. Pathol.* **170**, 1200–1209
28. Guo, H., Albrecht, S., Bourdeau, M., Petzke, T., Bergeron, C., and LeBlanc, A. C. (2004) Active caspase-6 and caspase-6-cleaved tau in neuropil threads, neuritic plaques, and neurofibrillary tangles of Alzheimer's disease. *Am. J. Pathol.* **165**, 523–531
29. Sperber, B. R., Leight, S., Goedert, M., and Lee, V. M. (1995) Glycogen synthase kinase-3 beta phosphorylates tau protein at multiple sites in intact cells. *Neurosci. Lett.* **197**, 149–153
30. Evans, D. B., Rank, K. B., Bhattacharya, K., Thomsen, D. R., Gurney, M. E., and Sharma, S. K. (2000) Tau phosphorylation at serine 396 and serine 404 by human recombinant tau protein kinase II inhibits tau's ability to promote microtubule assembly. *J. Biol. Chem.* **275**, 24977–24983
31. Lippa, C. F., Nee, L. E., Mori, H., and St George-Hyslop, P. (1998) Abeta-42 deposition precedes other changes in PS-1 Alzheimer's disease. *Lancet* **352**, 1117–1118
32. Oddo, S., Caccamo, A., Kitazawa, M., Tseng, B. P., and LaFerla, F. M. (2003) Amyloid deposition precedes tangle formation in a triple transgenic model of Alzheimer's disease. *Neurobiol. Aging* **24**, 1063–1070
33. Holmes, C., Boche, D., Wilkinson, D., Yadegarfar, G., Hopkins, V., Bayer, A., Jones, R. W., Bullock, R., Love, S., Neal, J. W., Zotova, E., and Nicoll, J. A. (2008) Long-term effects of Abeta42 immunisation in Alzheimer's disease: follow-up of a randomised, placebo-controlled phase I trial. *Lancet* **372**, 216–223
34. Arendash, G. W., Lewis, J., Leighty, R. E., McGowan, E., Cracchiolo, J. R., Hutton, M., and Garcia, M. F. (2004) Multi-metric behavioral comparison of APPsw and P301L models for Alzheimer's disease: linkage of poorer cognitive performance to tau pathology in forebrain. *Brain Res.* **1012**, 29–41
35. Yoshiyama, Y., Higuchi, M., Zhang, B., Huang, S. M., Iwata, N., Saido, T. C., Maeda, J., Suhara, T., Trojanowski, J. Q., and Lee, V. M. (2007) Synapse loss and microglial activation precede tangles in a P301S tauopathy mouse model. *Neuron* **53**, 337–351
36. Ramsden, M., Kotilinek, L., Forster, C., Paulson, J., McGowan, E., SantaCruz, K., Guimaraes, A., Yue, M., Lewis, J., Carlson, G., Hutton, M., and Ashe, K. H. (2005) Age-dependent neurofibrillary tangle formation, neuron loss, and memory impairment in a mouse model of human tauopathy (P301L). *J. Neurosci.* **25**, 10637–10647
37. Dickey, C. A., Kamal, A., Lundgren, K., Klosak, N., Bailey, R. M., Dunmore, J., Ash, P., Shoraka, S., Zlatkovic, J., Eckman, C. B., Patterson, C., Dickson, D. W., Nahman, N. S., Jr., Hutton, M., Burrows, F., and Petrucelli, L. (2007) The high-affinity HSP90-CHIP complex recognizes and selectively degrades phosphorylated tau client proteins. *J. Clin. Invest.* **117**, 648–658
38. Dickey, C. A., Dunmore, J., Lu, B., Wang, J. W., Lee, W. C., Kamal, A., Burrows, F., Eckman, C., Hutton, M., and Petrucelli, L. (2006) HSP induction mediates selective clearance of tau phosphorylated at proline-directed Ser/Thr sites but not KXGS (MARK) sites. *FASEB J.* **20**, 753–755
39. Ishizawa, T., Sahara, N., Ishiguro, K., Kersh, J., McGowan, E., Lewis, J., Hutton, M., Dickson, D. W., and Yen, S. H. (2003) Co-localization of glycogen synthase kinase-3 with neurofibrillary tangles and granulovacuolar degeneration in transgenic mice. *Am. J. Pathol.* **163**, 1057–1067
40. Ter Haar, E., Coll, J. T., Austen, D. A., Hsiao, H. M., Swenson, L., and Jain, J. (2001) Structure of GSK3beta reveals a primed phosphorylation mechanism. *Nat. Struct. Biol.* **8**, 593–596
41. Sayas, C. L., Ariaens, A., Ponsioen, B., and Moolenaar, W. H. (2006) GSK-3 is activated by the tyrosine kinase Pyk2 during LPA1-mediated neurite retraction. *Mol. Biol. Cell* **17**, 1834–1844
42. Lesort, M., Jope, R. S., and Johnson, G. V. (1999) Insulin transiently increases tau phosphorylation: involvement of glycogen synthase kinase-3beta and Fyn tyrosine kinase. *J. Neurochem.* **72**, 576–584
43. Yusta, B., Estall, J., and Drucker, D. J. (2002) Glucagon-like peptide-2 receptor activation engages bad and glycogen synthase kinase-3 in a protein kinase A-dependent manner and prevents apoptosis following inhibition of phosphatidylinositol 3-kinase. *J. Biol. Chem.* **277**, 24896–24906
44. Fang, X., Yu, S., Tanyi, J. L., Lu, Y., Woodgett, J. R., and Mills, G. B. (2002) Convergence of multiple signaling cascades at glycogen synthase kinase 3: edg receptor-mediated phosphorylation and inactivation by lysophosphatidic acid through a protein kinase C-dependent intracellular pathway. *Mol. Cell. Biol.* **22**, 2099–2110
45. Terwel, D., Muyliaert, D., Dewachter, I., Borghgraef, P., Croes, S., Devijver, H., and Van Leuven, F. (2008) Amyloid activates GSK-3beta to aggravate neuronal tauopathy in bigenic mice. *Am. J. Pathol.* **172**, 786–798
46. Bhaskar, K., Yen, S. H., and Lee, G. (2005) Disease-related modifications in tau affect the interaction between fyn and tau. *J. Biol. Chem.* **280**, 35119–35125
47. Lee, G., Thangavel, R., Sharma, V. M., Litersky, J. M., Bhaskar, K., Fang, S. M., Do, L. H., Andreadis, A., Van Hoesen, G., and Ksiazak-Reding, H. (2004) Phosphorylation of tau by fyn: implications for Alzheimer's disease. *J. Neurosci.* **24**, 2304–2312
48. Cho, J. H., and Johnson, G. V. (2004) Glycogen synthase kinase 3 beta induces caspase-cleaved tau aggregation in situ. *J. Biol. Chem.* **279**, 54716–54723

Received for publication November 25, 2009.

Accepted for publication February 25, 2010.